Uniport Journal of Engineering and Scientific Research (UJESR)

Vol. 9, Special Issue, 2024, Page 68-76
ISSN: 2616-1192

(www.ujesr.org)

© Faculty of Engineering, University of Port Harcourt, Nigeria.

Periodic Oscillations of a Truly Nonlinear Non-Natural Oscillator

Akuro Big-Alabo[1]*, [2]Joseph Chukwuka Ofodu
[1]Applied Mechanics & Design (AMD) Research Group, Department of Mechanical Engineering, Faculty of Engineering, University of Port Harcourt, Port Harcourt, Nigeria
[2]Energy and Thermofluid Engineering (ETE) Research Group, Department of Mechanical Engineering, Faculty of Engineering, University of Port Harcourt, Port Harcourt, Nigeria
*Correspondence Email: *akuro.big-alabo@uniport.edu.ng*

Abstract
In this paper, a Lienard-type second order ordinary differential equation representing a class of non-natural oscillators with truly nonlinear periodic response was proposed and investigated. These nonlinear oscillators are characterized by position-dependent mass and velocity-dependent elastic force, and they exhibit a strong nonlinear response for all amplitudes and values of the system parameters. It was shown that the well-known Mathews-Lakshmanan oscillator, which has application in relativistic mechanics, is a special case of the present model. The exact frequency-amplitude response and periodic solution for the non-natural oscillator model were derived in closed form in terms of the Euler-Gamma and incomplete Euler-Beta functions respectively. The phase response, frequency-amplitude response and displacement response were simulated for various ranges of the index of the conservative restoring force and it was confirmed that the oscillator exhibited strong nonlinear response for all values positive real values of the index except when the index is equal to 1 or 2.

Keywords: *non-natural oscillator, truly nonlinear oscillator, Mathews-Lakshmanan oscillator, Lienard-type oscillator, Euler-Beta function*

Received: 16th December, 2024 *Accepted: 31st December, 2024*

1. Introduction

Nonlinear oscillations are ubiquitous in nature and technological processes. In general, a nonlinear oscillating system can exhibit weak, moderate or strong nonlinear response depending on the amplitude of oscillation and the values of the system parameters. Such an oscillating system can be referred to as a generally nonlinear oscillator. Another type of oscillating system is one that always exhibits a strong nonlinear response irrespective of the amplitude of oscillation and the values of the system parameters. This type of oscillating system is referred to as a truly nonlinear oscillator (Mickens, 2010) or pure nonlinear oscillator (Cveticanin, 2018). Examples of truly nonlinear oscillations exist in the oscillations of ball-bearing in a cylindrical glass tube (He, 2002), oscillations of an electron beam in a magnetically-charged plasma tube (He, 2006), and vibrating systems with fractional order nonlinear restoring force (Cveticanin and Pogany, 2018)..

Truly nonlinear oscillations have been long investigated for natural oscillations but these have not been investigated for non-natural oscillations. The latter have the advantage of incorporating variable and dynamic inertia effects, which are not accounted for in natural oscillations. Variable and dynamic inertia effects exist in macro-scale mechanical vibrations (e.g. beams carrying intermediate mass (Big-Alabo et al., 2020a), liquid sloshing in elliptic tanks (Zheng et al., 2012), porter governor (Parnaby and Porter, 1968; Big-Alabo et al., 2021a), slider-crank mechanism (Big-Alabo et al., 2020b) and bifilar pendulum (Ulher, 1923)) and in micro-scale particle oscillations (e.g. particle on a rotating parabola (Nayfeh and Mook, 1995), phase transition (Lev et al., 2017; Big-Alabo et al., 2021b) and relativistic mechanics (Mathews and Lakshmanan, 1974)). Therefore, this paper presents a new model for a class of non-natural oscillators that exhibit truly nonlinear oscillations. The present model is characterized by a position-dependent mass (or variable inertia), velocity-dependent elastic force (or dynamic inertia) and a static elastic force. The well-known Mathews-Lakshmanan (M-L) oscillator is a special case of the present non-natural

oscillator model. The exact periodic solution of the present model was derived in closed form and some interesting qualitative features of the model were discussed.

2. Mathematical model

Let us consider a class of strong nonlinear oscillators of the Lienard-type that are governed by differential equations of the form:

$$I(s)\ddot{s} - \frac{1}{2}I'(s)\dot{s}^2 + \rho I'(s) = 0 \quad (1)$$

where $I(s)$ is the effective inertia of the oscillator which varies with position, the prime and dot represents differentiation with respect to s and t respectively, and the initial conditions are $s(0) = A$ and $\dot{s}(0) = 0$. This class of nonlinear oscillators are characterized by position-dependent mass (or variable inertia) and dynamic inertia nonlinearity. They represent a wide range of systems in physics and engineering, and have applications in the study of optical and electronic structures of semi-conductors (Von Roos, 1983), super-lattice band structures (Karthiga et al., 2017) and quantum mechanical systems (Cruz-y-Cruz et al., 2007). The second term of the Equation (1) is a quadratic damping term that does not produce a dissipative effect but acts as a dynamic restoring force. Hence, the total restoring force is the sum of this dynamic force and the static restoring force (i.e. the third term in the equation), and can be expressed as:

$$g(s,\dot{s}) = \frac{2\rho I'(s) - I'(s)\dot{s}^2}{2I(s)} \quad (2)$$

The total restoring force gives rise to conservation of the energy of the system and is therefore referred to as the 'conservative' restoring force.

Nonlinear oscillators in which the conservative restoring force has a velocity squared term are referred to as non-natural oscillators (Nayfeh and Mook, 1995). Big-Alabo (2020a) studied the periodic solution and qualitative response of non-natural systems based on their restoring force. It was shown that a non-natural oscillator governed by a differential equation of the form:

$$I(s)\ddot{s} + kI'(s)\dot{s}^2 = Q(s) \quad (3)$$

has a conservative restoring force expressible as an explicit function of the spatial variable as follows:

$$g(s) = \frac{2kI'(s)[h(A) - h(s)]}{[I(s)]^{2k+1}} - \frac{Q(s)}{I(s)} \quad (4)$$

where $h(s) = -\int [I(s)]^{2k-1} Q(s)du$. For Equation (1), $k = -1/2$ and $Q(s) = -\rho I'(s)$. Therefore, the conservative restoring force can be written in terms of the spatial variable as:

$$g(s) = \frac{\rho}{I(A)}I'(s) \quad (5)$$

Then, Equation (1) can be rewritten in equivalent conservative form as:

$$\ddot{s} + \frac{\rho}{I(A)}I'(s) = 0 \quad (6)$$

Equation (6) can only have periodic solutions when $I(s)$ is nonlinear. In general, a nonlinear $I(s)$ can produce an oscillator with weak or strong nonlinear response depending on the values of the oscillation amplitude and system parameters. However, the focus of the present study is on truly nonlinear non-natural oscillators that are characterized by strong nonlinearity for all amplitudes and values of the system parameters. To this end, the variable inertia is defined as $I(s) = \alpha + \beta s^m$ where $m > 0$ and $m \neq 1$. This model of the variable inertia produces a class of non-natural oscillators that will exhibit a truly nonlinear response for all m except for $m = 2$. Therefore, the governing model for the present truly nonlinear non-natural oscillator is:

$$(\alpha + \beta s^m)\ddot{s} - \frac{1}{2}\beta m s^{m-1}\dot{s}^2 + \rho\beta m s^{m-1} = 0 \quad (7)$$

and the corresponding Lagrangian is:

$$\mathcal{L} = \frac{1}{2}\left[\frac{\alpha\dot{s}^2 - 2\rho\beta s^m}{\alpha(\alpha + \beta s^m)}\right] \quad (8)$$

where the kinetic and potential energies are $T = \frac{1}{2}(\alpha + \beta s^m)^{-1}\dot{s}^2$ and $U = \rho\beta s^m/[\alpha(\alpha + \beta s^m)]$ respectively. Equation (8) is the Lagrangian density analogue of a class of relativistic scalar fields that are applicable to pion interactions (Mathews and Lakshmanan, 1974). The case of $m = 2$ gives a non-natural oscillator characterized by purely harmonic oscillations and is known as the Mathews-Lakshmanan oscillator. The M-L oscillator is useful for investigating oscillations arising in high-energy quantum-mechanical particle motion (Mathews and Lakshmanan, 1974) and is a special case of Equation (7). Substituting $I(s) = \alpha + \beta s^2$ in Equation (6), the M-L oscillator can be express as:

$$\ddot{s} + \left(\frac{2\rho\beta}{\alpha + \beta A^2}\right)s = 0, \quad (9)$$

where the solution to Equation (9) is $s(t) = A\cos\omega t$ and $\omega = \sqrt{2\rho\beta/(\alpha + \beta A^2)}$ is the natural frequency, which depends on the amplitude. For the classical M-L oscillator [15], $\alpha = 1$ and $\Lambda = 2\rho\beta$. On one hand, all periodic solutions of the M-L oscillator are simple harmonic, which is a quality of linear oscillators. On the other hand, its natural frequency is amplitude dependent, which is a quality of nonlinear oscillators. However, the M-L oscillator is characterized by a weak nonlinear response when $\beta A^2 \ll \alpha$ and a strong nonlinear

response otherwise. This means that the M-L oscillator is not a truly nonlinear oscillator.

Substituting $I(s) = \alpha + \beta s^m$ in Equation (6) gives the equivalent conservative form for Equation (7) as:

$$\ddot{s} + \left(\frac{m\rho\beta}{\alpha + \beta A^m}\right) s^{m-1} = 0, \tag{10}$$

which describes the oscillations of a truly nonlinear oscillator with amplitude-dependent stiffness provided $m > 0$ and $m \neq \{1,2\}$. Note that periodic solutions do not exist for $m \leq 0$ and $m = 1$. When $m = 0$, the response of the system is that of a rectilinear motion with constant velocity while $m = 1$ gives a rectilinear motion with constant deceleration. The values $m = 3$, 4 and 6 produces the purely quadratic, cubic and quintic nonlinear oscillators respectively, while $m = 4/3$ gives the well-studied $1/3$ fractional power oscillator. All these oscillators have exact periodic solutions in terms of elliptic functions (Mickens, 2010; Cveticanin, 2018).

3. Closed-form solution

In this section, the exact closed-form solution to Equation (10) was derived.

3.1. Frequency-amplitude response of the truly nonlinear non-natural oscillator

The energy-balance of Equation (10) can be derived by pre-multiplying by $\dot{s}$ and then integrating to get:

$$\frac{1}{2}\dot{s}^2 + \left(\frac{\rho\beta}{\alpha + \beta A^m}\right) s^m = \left(\frac{\rho\beta}{\alpha + \beta A^m}\right) A^m \tag{11}$$

from which the time period can be evaluated by the following integral:

$$T_{ex} = 4\sqrt{\frac{\alpha + \beta A^m}{2\rho\beta A^m}} \int_0^A \frac{ds}{\sqrt{1 - (s/A)^m}} \tag{12}$$

Using the transformed variable $x = (s/A)^m$ in Equation (12) gives:

$$T_{ex} = \frac{4A}{m}\sqrt{\frac{\alpha + \beta A^m}{2\rho\beta A^m}} \int_0^1 x^{(1-m)/m}(1-x)^{-1/2} dx \tag{13}$$

Therefore,

$$T_{ex} = \frac{4A}{m}\sqrt{\frac{\alpha + \beta A^m}{2\rho\beta A^m}}\, B\left(\frac{1}{m}, \frac{1}{2}\right) \tag{14}$$

where the Euler-Beta function is defined as:

$$B(p,q) = \int_0^1 x^{p-1}(1-x)^{q-1} dx \tag{15}$$

Finally, by noting that $B(p,q) = B(q,p)$ and exploiting the Legendre duplication formula for the Euler-Beta function, i.e.

$$B\left(\frac{1}{2}, p\right) = \frac{2^{2p-1}\Gamma^2(p)}{\Gamma(2p)} \tag{16}$$

the exact time period was derived in terms of the Euler-Gamma function as:

$$T_{ex} = \frac{2^{(2+m)/m} A^{(2-m)/2}}{m}\sqrt{\frac{\alpha + \beta A^m}{2\rho\beta}}\frac{\Gamma^2(1/m)}{\Gamma(2/m)} \tag{17}$$

where $\Gamma^2(p) = \left(\Gamma(p)\right)^2$. The Euler-Gamma function for any rational number can be evaluated accurately using the **Gamma [·]** function in Mathematica™ computational package. Substituting $m = 2$ in Equation (17) gives $T_{ex} = 2\pi\sqrt{(\alpha + \beta A^2)/2\rho\beta}$, which is the exact period for the M-L oscillator in Equation (9).

Hence, the exact frequency-amplitude response can be obtained from Equation (17) as shown in Equation (18).

$$\Omega_{ex} = \frac{m\pi}{4^{1/m} A^{(2-m)/2}}\sqrt{\frac{2\rho\beta}{\alpha + \beta A^m}}\frac{\Gamma(2/m)}{\Gamma^2(1/m)} \tag{18}$$

3.2. Displacement solution of the truly nonlinear non-natural oscillator

The exact displacement history of the first quarter of the oscillation cycle (i.e. $A \geq s \geq 0$) can be obtained from Equation (11) as follows:

$$t = \sqrt{\frac{\alpha + \beta A^m}{2\rho\beta A^m}} \int_s^A \frac{dr}{\sqrt{1 - (r/A)^m}}$$

$$= \frac{1}{4}T_{ex} - \sqrt{\frac{\alpha + \beta A^m}{2\rho\beta A^m}} \int_0^s \frac{dr}{\sqrt{1 - (r/A)^m}} \tag{19}$$

After transformation,

$$\int_0^s \frac{dr}{\sqrt{1 - (r/A)^m}}$$

$$= \frac{A}{m}\int_0^{\psi(s)} x^{(1-m)/m}(1-x)^{-1/2} dx \tag{20}$$

where $\psi(s) = (|s|/A)^m$. The integral on the right hand side of Equation (20) is the incomplete Euler-Beta function defined as:

$$B(\theta; p, q) = \int_0^\theta x^{p-1}(1-x)^{q-1} dx \tag{21}$$

Therefore,

$$t = \frac{1}{4}T_{ex} - \frac{A}{m}\sqrt{\frac{\alpha + \beta A^m}{2\rho\beta A^m}}\, B\left(\left(\frac{|s|}{A}\right)^m; \frac{1}{m}, \frac{1}{2}\right) \tag{22}$$

The incomplete Euler-Beta function can be accurately evaluated using the built-in **Beta [· , · , ·]** function in Mathematica™ computational package. Therefore, for a given displacement, the corresponding time can be computed, thereby providing displacement-time data for plotting the

displacement profile. A similar approach for plotting the exact displacement-time graph of non-natural oscillators can be found in the references (Big-Alabo et al., 2021b; Big-Alabo, 2021).

The corresponding solutions for the remaining three quarters of the oscillation cycle are:
Second quarter (i.e. $0 \geq s \geq -A$),

$$t = \frac{1}{4}T_{ex} + \frac{A}{m}\sqrt{\frac{\alpha+\beta A^m}{2\rho\beta A^m}}\,B\left(\left(\frac{|s|}{A}\right)^m;\frac{1}{m},\frac{1}{2}\right) \quad (23)$$

Third quarter (i.e. $-A \leq s \leq 0$),

$$t = \frac{3}{4}T_{ex} - \frac{A}{m}\sqrt{\frac{\alpha+\beta A^m}{2\rho\beta A^m}}\,B\left(\left(\frac{|s|}{A}\right)^m;\frac{1}{m},\frac{1}{2}\right) \quad (24)$$

Fourth quarter (i.e. $0 \leq s \leq A$),

$$t = \frac{3}{4}T_{ex} + \frac{A}{m}\sqrt{\frac{\alpha+\beta A^m}{2\rho\beta A^m}}\,B\left(\left(\frac{|s|}{A}\right)^m;\frac{1}{m},\frac{1}{2}\right) \quad (25)$$

Alternatively, the displacement solution can be expressed in terms of the Ateb function. Cveticanin (2018) showed that the solution to the truly nonlinear oscillator of the form:

$$\ddot{x} + c_\sigma^2 x|x|^{\sigma-1} = 0 \quad (26)$$

with initial condition $x(0) = A$ and $\dot{x}(0) = 0$, can be derived as:

$$x(t) = A \times ca\left(\sigma, 1, c_\sigma\sqrt{\frac{\sigma+1}{2}}A^{(\sigma-1)/2}t\right) \quad (27)$$

where ca is the cosine Ateb function which can be evaluated in terms of Fourier series (Cveticanin, 2018) or numerically (Cveticanin and Pogany, 2012). Now comparing Equations (10) and (26), $\sigma = m-1$, $c_\sigma^2 = m\rho\beta/(\alpha+\beta A^m)$ and $s(t) \equiv x(t)$. Therefore, the displacement solution of the truly nonlinear non-natural oscillator in Equation (10) can be expressed in terms of Ateb function as:

$$s(t) = A \times ca\left(m-1, 1, mA^{\left(\frac{m-2}{2}\right)}\sqrt{\frac{\rho\beta}{2(\alpha+\beta A^m)}}t\right) \quad (28)$$

For $m = 2$,

$$s(t) = A \times ca\left(1, 1, \sqrt{\frac{2\rho\beta}{\alpha+\beta A^2}}t\right)$$

$$= A\cos\left(\sqrt{\frac{2\rho\beta}{\alpha+\beta A^2}}t\right) \quad (29)$$

since $ca(1,1,z) = \cos z$. Equation (29) is the same as the exact displacement solution of the M-L oscillator, which is a special case of the present model when $m = 2$.

4. Results and discussions

The following input values were used for all simulations except otherwise stated: $\alpha = 1.0$, $\beta = 1.0$, $\rho = 1.0$, and $A = 1.0$.

4.1. Phase portraits and displacement response

The phase equation for the truly nonlinear non-natural oscillator can be derived from the energy-balance equation in Equation (11) as shown:

$$\dot{s}(s) = \pm\sqrt{\frac{2\rho\beta(A^m - |s|^m)}{\alpha+\beta A^m}} \quad (30)$$

Phase portraits for the truly nonlinear non-natural oscillator were plotted over a half-plane as shown in Figures 1 to 3. Three cases are considered for which

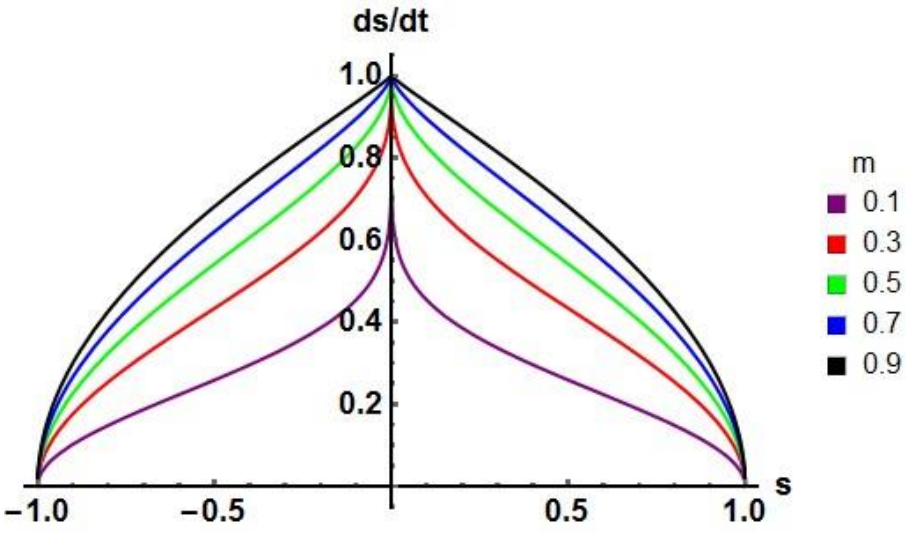

Fig. 1: Half-plane phase portrait of truly nonlinear non-natural oscillator when $0 < m < 1.0$.

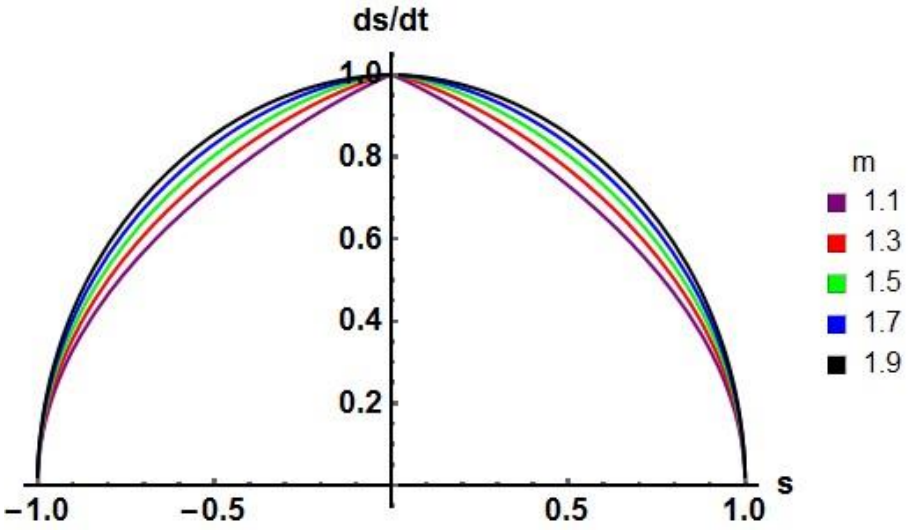

Fig. 2: Half-plane phase portrait of truly nonlinear non-natural oscillator when $1.0 < m < 2.0$.

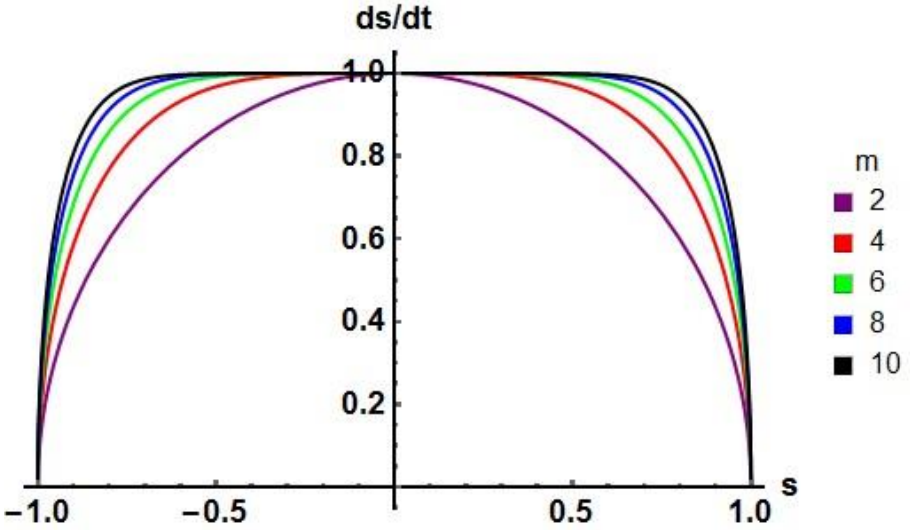

Fig. 3: Half-plane phase portrait of truly nonlinear non-natural oscillator when $m \geq 2.0$

periodic solutions exist based on the nonlinear index: (a) $0 < m < 1.0$ (see Figure 1) (b) $1.0 < m < 2.0$ (see Figure 2) and (c) $m \geq 2.0$ (see Figure 3). Outside these ranges, there are no periodic solutions. However, truly nonlinear oscillations occur for all cases in these ranges except for $m = 2$, for which the oscillations are generally nonlinear.

The phase portraits show that the system exhibits strong anharmonic response for $0 < m < 1.0$ and for $m \gg 2$. When $m \approx 2$, the phase portrait is almost a circle and the system response is basically harmonic. Hence, systems having $m \approx 2$ can be investigated using the M-L oscillator. Another observation is that the phase portrait takes an approximately rectangular shape for very large m (see Figure 3). The system maintains a constant velocity that alternates its sign over each half-cycle. In such cases, the system behaves as a light photon moving in straight paths while oscillating.

The displacement responses for the three cases of the nonlinear index are shown Figures 4 to 6. It can be seen that the period of oscillation decreases with increase in the nonlinear index for each of the three cases. The displacement response for $0 < m < 1.0$ does not show clearly the anharmonicity in the system response. The anharmonicity is rather seen in the velocity response as illustrated in Figure 7. As m gets closer to zero, there is a sudden spike in the velocity response at the equilibrium points where the displacement is zero. On the other hand, as m gets closer to 1, the velocity produces a linear response and a sudden change in direction around its turn points. For $m \gg 2$, the anharmonicity in the system's response is obvious in the displacement response and increases with increase in m. An asymptotic response was observed for very large m, and this response has similar characteristics as the response of a light photon (Big-Alabo, 2020b) i.e. a

saw-tooth wave for the displacement response and a rectangular wave for the velocity response.

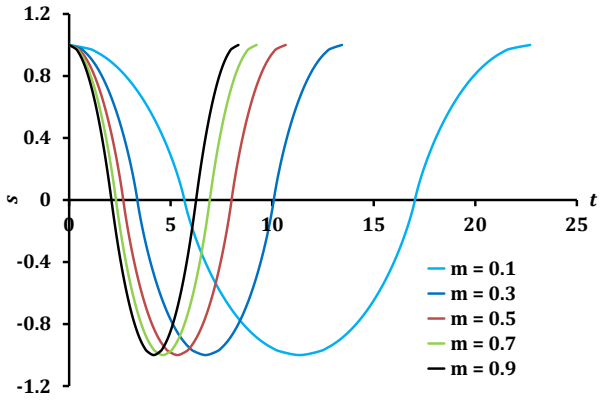

Fig. 4: Displacement response for $0 < m < 1.0$.

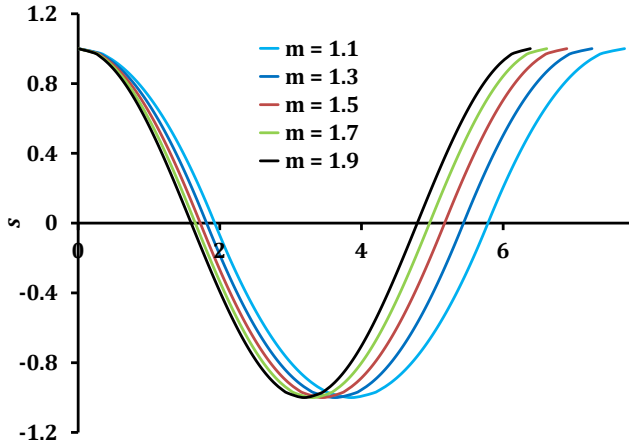

Fig. 5: Displacement response for $1.0 < m < 2.0$.

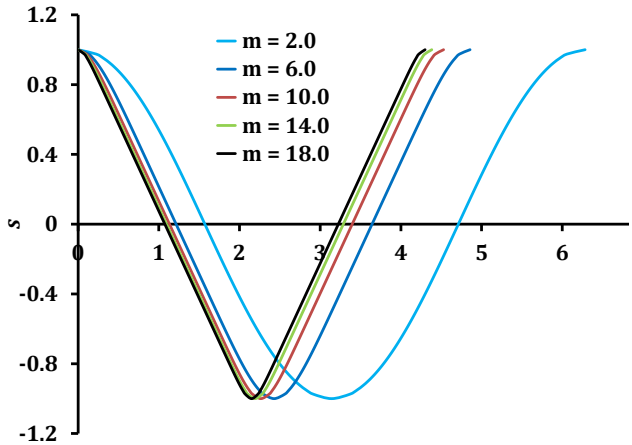

Fig. 6: Displacement response for $m \geq 2.0$.

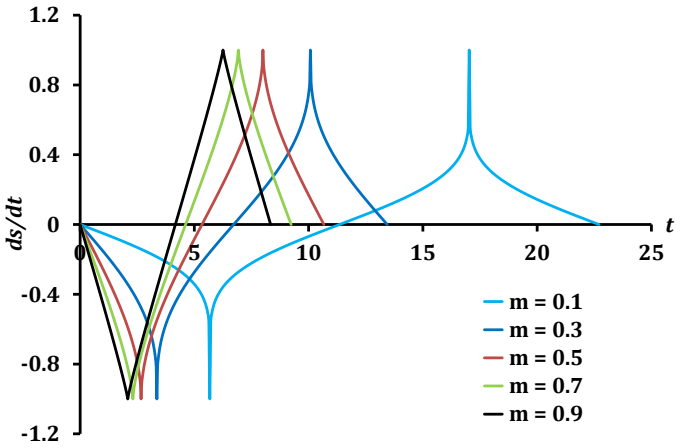

Fig. 7: Velocity response for $0 < m < 1.0$.

4.2. Frequency-amplitude response

Results of the frequency-amplitude for different values of the system parameters and oscillation amplitude were plotted in Figures 8 to 12. Again, the three cases of the nonlinear index were considered in investigating the frequency-amplitude response. Figure 8 shows the dependence of the nonlinear frequency on the amplitude when the nonlinear index is less than 1.0. A strong dependence was observed for small-amplitude oscillations whereas the nonlinear frequency becomes negligible and approaches an asymptotic value of $\Omega_{ex} \to 0$ in the large-amplitude domain.

Figures 9 and 10 are plots showing the dependence of natural frequency on the amplitude when the nonlinear index is greater than 1. Two cases were considered namely: (a) $1.0 < m \leq 2.0$ (see Figure 9) and (b) $m > 2.0$ (see Figure 10). In Figure 9, a strong dependence was observed for small amplitudes but a gradual variation of frequency with the nonlinear index occurred at large amplitudes. The frequency decreased with increase in the nonlinear index and the amplitude of oscillation. In Figure 10, the frequency increased initially with increase in amplitude until some critical amplitude was attained, beyond which the frequency decreased with increase in amplitude. On the other hand, the frequency decreased with increase in the nonlinear index when the amplitude is less than the critical amplitude, while the opposite response was observed beyond the critical amplitude. Although, the physical significance of the critical amplitude does not seem obvious in the course of this investigation, it may be worthwhile to investigate it further in future studies.

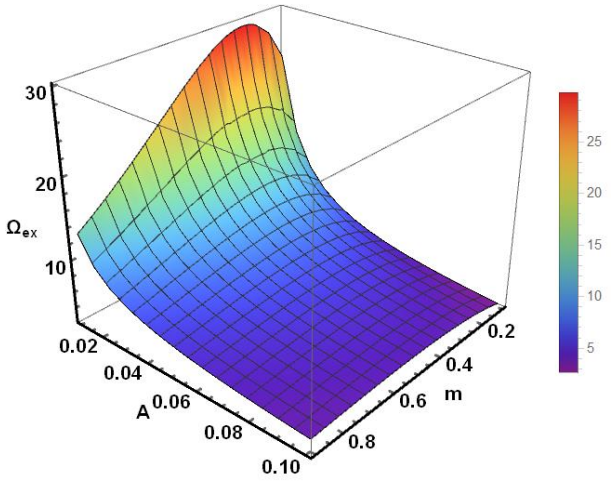

Top plot

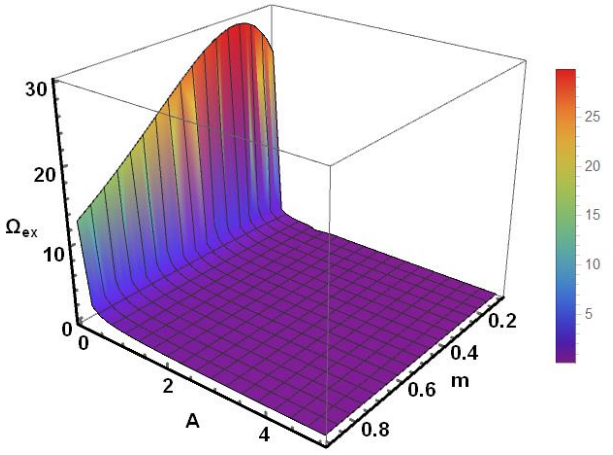

Bottom plot

Fig. 8: Variation of nonlinear frequency with amplitude and nonlinear index for $0 < m < 1.0$. Top plot $(0.01 \leq A \leq 0.1)$; Bottom plot $(0.01 \leq A \leq 5.0)$

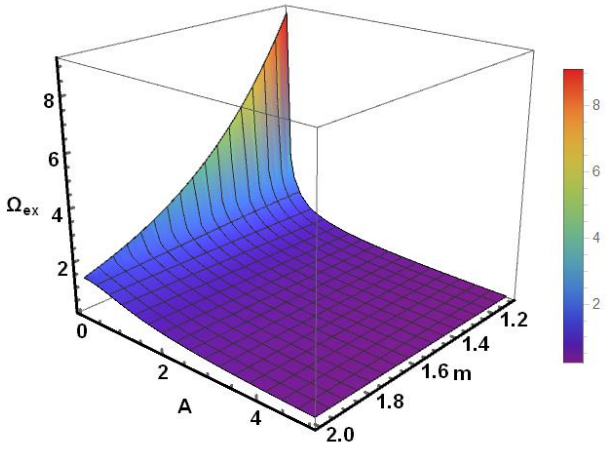

Fig. 9: Variation of nonlinear frequency with amplitude and nonlinear index for $1.0 < m \leq 2.0$ and $0.01 \leq A \leq 5.0$.

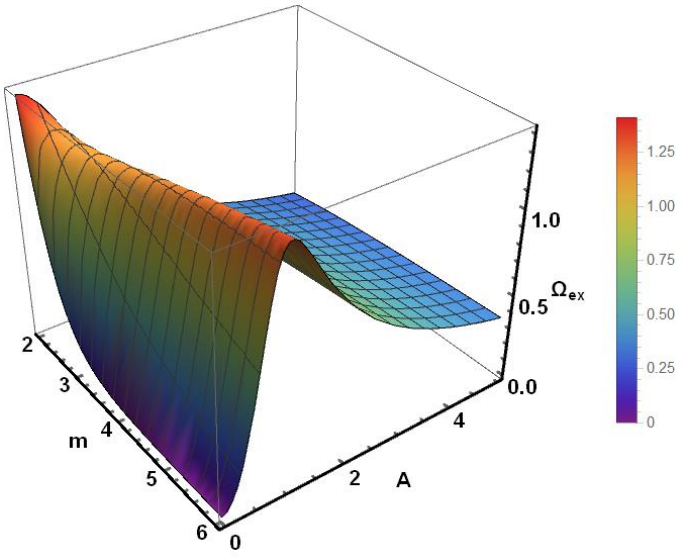

Fig. 10: Variation of nonlinear frequency with amplitude and nonlinear index for $2.0 < m \leq 6.0$ and $0.01 \leq A \leq 5.0$.

Figure 11 illustrates the dependence of the nonlinear frequency on the static nonlinear stiffness and the nonlinear index for small and large amplitude responses. For the small amplitude response, the frequency was observed to increase with increase in the static nonlinear stiffness for $m > 2.0$ and decrease with increase in the nonlinear index. Thie frequency was seen to be insensitive to the static nonlinear stiffness for larger values of the nonlinear index. However, for the large amplitude response, the frequency was observed to increase with increase in the static nonlinear stiffness and the nonlinear index.

Figure 12 shows the variation of the nonlinear frequency with inertia nonlinearity and nonlinear index for small and large amplitude responses when $m > 2$. The small amplitude frequency response for the inertia nonlinearity seems to be similar to the corresponding response for the static nonlinear stiffness, which implies that static and inertia nonlinearities have similar effect on the frequency response during small amplitude oscillation when $m > 2$. However, the large amplitude response showed that the frequency is insensitive to the change in the inertia nonlinearity and increases with increase in order of nonlinearity. This behaviour is in stark contrast to the frequency dependence on static nonlinearity during large amplitude response.

5. Conclusion

A truly nonlinear non-natural oscillator model of the Lienard-type that has application in physics, engineering and technological processes, and is characterized by variable and dynamic inertia

effects have been proposed in this study. The well-known Mathews-Lakshmanan oscillator in particle physics is a special case of the present model. It was shown that the present non-natural oscillator is characterized by pure nonlinearity with amplitude-dependent stiffness. The exact frequency-amplitude response and displacement solutions were derived in closed-form in terms of the Euler-Gamma (or Euler-Beta) and the incomplete Euler-Beta functions.

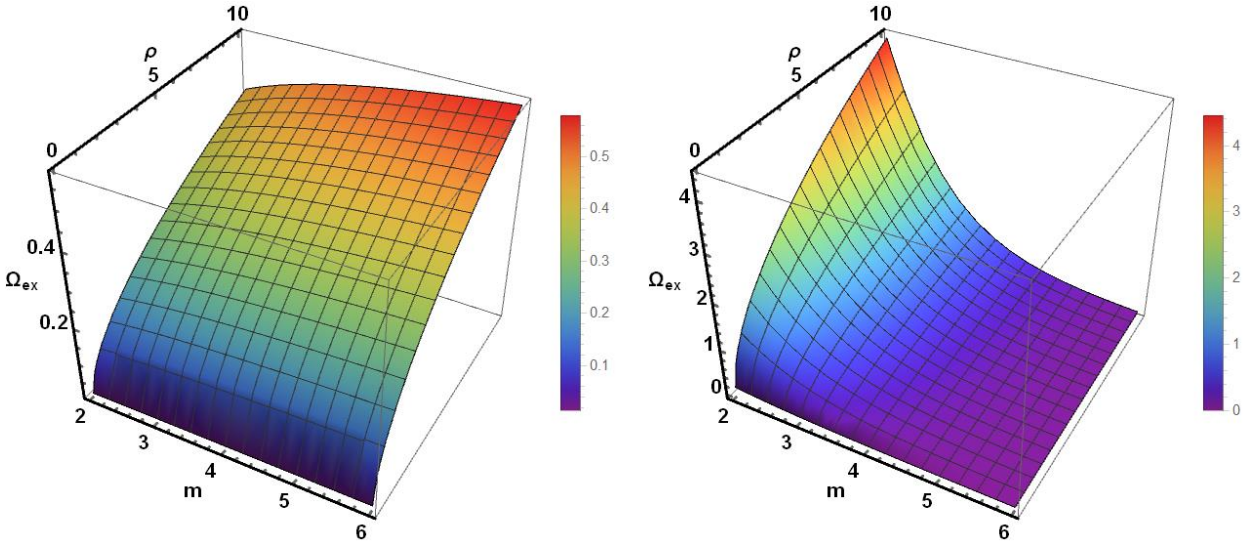

Fig. 11: Variation of nonlinear frequency with static nonlinear stiffness and nonlinear index for $2.0 < m \leq 6.0$ and $0.01 \leq \rho \leq 10.0$. Left: small amplitude response ($A = 0.10$) and right: large amplitude response ($A = 10.0$).

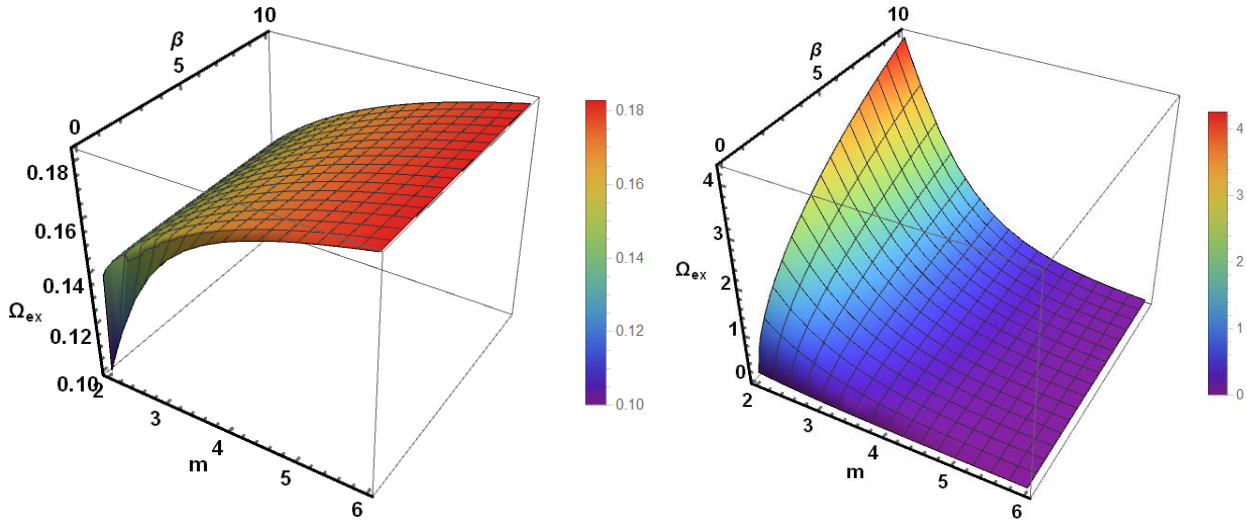

Fig. 12: Variation of nonlinear frequency with nonlinear inertia stiffness and nonlinear index for $2.0 < m \leq 6.0$ and $0.01 \leq \beta \leq 10.0$. Left: small amplitude response ($A = 0.10$) and right: large amplitude response ($A = 10.0$).

The results showed that the nonlinear frequency depends strongly on the system parameters, the amplitude of oscillation and the nonlinear index. However, at very large amplitudes it was observed that the frequency response was generally insensitive to changes in the nonlinear index. It was also observed that the effects of static nonlinearity and inertia nonlinearity on the frequency response during small amplitude oscillations were similar when $m > 2$. In contrast, the static nonlinear effect was significantly different from the inertia nonlinear effect during large amplitude oscillations. Results of the displacement response reveal the existence of an asymptotic response for very large values of the nonlinear index and this asymptotic response is similar to the ultra-relativistic response of the

simple harmonic relativistic oscillator. Finally, this study presents a unique oscillator model with potential application in the study of nano-scale systems where the mass is position dependent (Karthiga et al., 2017). Further studies can be conducted on the qualitative response of the system to determine the conditions for chaotic response. Also, approximate analytical solutions can be explored.

Declaration of conflicting interests

None declared.

Data availability statement

All necessary data for this study has been included in the manuscript.

Funding/acknowledgement

This article is dedicated to honouring Prof Joseph A Ajienka on the occasion of his retirement and 70th birthday.

References

Big-Alabo, A (2020a). Approximate periodic solution and qualitative analysis of non-natural oscillators based on the restoring force, Engineering Research Express, 2(1), 015029.

Big-Alabo, A (2020b). Continuous piecewise linearization method for approximate periodic solution of the relativistic oscillator, International Journal of Mechanical Engineering Education, 48(2), 178-194.

Big-Alabo, A (2021). Exact analysis of the nonlinear vibration of an achetypal non-natural oscillator, European Physical Journal Plus, 136(1):107, 1-17.

Big-Alabo, A, Ekpruke, EO, Ossia, CV (2021a). Equivalent oscillator model for the nonlinear vibration of a porter governor, Journal of King Saud University - Engineering Sciences, DOI:10.1016/j.jksues.2021.01.009.

Big-Alabo, A, Ogbodo, CO, Ossia, CV (2020b). Semi-analytical treatment of complex nonlinear oscillations arising in the slider-crank mechanism, World Scientific News, 142, 1-24.

Big-Alabo, A, Ossia, CV, Ekpruke, EO (2021b). Exact analytical solution of a mechanical oscillator for phase transition involving spatially inhomogeneous distribution of the order parameter, Mathematical Methods in the Applied Sciences, DOI:10.1002/mma.7089.

Big-Alabo, A, Ossia, CV, Ekpruke, EO, Ogbonnia, CD (2020a). Large-amplitude vibration analysis of a strong nonlinear tapered beam using continuous piecewise linearization method, Journal of King Saud University - Engineering Sciences, DOI:10.1016/j.jksues.2020.11.005.

Cruz-y-Cruz, S, Negro, J, Nieto, LM (2007). Classical and quantum position-dependent mass harmonic oscillators, Physics Letters A, 369(5-6), 400-406.

Cveticanin, L and Pogany, T (2012). Oscillator with a sum of non-integer order non-linearities, Journal of Applied Mathematics, 649050, 20 pp.

Cveticanin, L (2018). Strong Nonlinear Oscillators: Analytical Solutions, 2nd Edition, Springer, Switzerland, 17-48.

He, JH (2002). Preliminary report on the energy balance for nonlinear oscillations, Mechanics Research Communications, 29, 107–111.

He, JH (2006). Some asymptotic methods for strongly nonlinear equations, International Journal of Modern Physics B, 20(10), 1141-1199.

Karthiga, S, Chithiika Ruby, V, Senthilvelan, M, Lakshmanan, M (2017). Quantum solvability of a general ordered position dependent mass system: Mathews-Lakshmanan oscillator, Journal of Mathematical Physics, 58, 102110.

Lev, BI, Tymchyshyn, VB, Zagorodny, AG (2017). On certain properties of nonlinear oscillator with coordinate-dependent mass. Phys. Lett. A 381(34), 17–23.

Mathews, PM, Lakshmanan, M (1974). On a unique nonlinear oscillator, Quarterly Applied Mathematics, 32, 215–218.

Mickens, RE (2010). Truly nonlinear oscillations: harmonic balance, parameter expansions, iteration, and averaging methods, World Scientific Publishing, Massachussets, 1-20.

Nayfeh, AH, Mook, DT (1995). Nonlinear Oscillations, Wiley, New York.

Parnaby, J and Porter, B (1968). Non-linear vibrations of a centrifugal governor. Int. J. Mech. Sci. 10, 187–200.

Uhler, HS (1923). Period of the bifilar pendulum for large amplitudes, Journal of Optical Society of America, 7, 263–269.

Von Roos, O (1983). Position-dependent effective masses in semiconductor theory, Physics Review B, 27, 7547.

Zheng, XL, Li, XS, and Ren, YY (2012). Equivalent mechanical model for lateral liquid sloshing in partially filled tank vehicles. Math. Probl. Eng. Article ID: 162825.